

**Light-curves of symbiotic stars in massive photometric surveys I:
D-type systems**M. Gromadzki¹, J. Mikołajewska¹,
P. Whitelock^{2,3}, F. Marang²¹N. Copernicus Astronomical Center, Bartycka 18, PL-00-716 Warsaw, Poland
e-mail: marg.mikolaj@camk.edu.pl²South African Astronomical Observatory, P.O. Box 9, Observatory, 7935, South Africa
e-mail: paw,fm@sao.ac.za³National Astrophysics and Space Science Programme, Department of Astronomy,
University of Cape Town, Rondebosch, 7701, South Africa*Received Month Day, Year*

ABSTRACT

ASAS, MACHO, OGLE and SAAO *JHKL* light curves of 13 stars, that have at some time been classified as D-type symbiotics, are analysed. Most of the near-IR light-curves that have been monitored over many years show long-term changes due to variable dust obscuration, in addition to the stellar pulsation. The distances to these objects are derived from the period-luminosity relation and estimates of the mass-loss rates made from the $K_0 - [12]$ colour.

We reclassify AS 245 as an S-type symbiotic, with a semi-regular cool component with a pulsation period of about one year. The periods of the large amplitude pulsations of SS73 38 (463 days), AS 210 (423 days) and H2-38 (395 days) are estimated for the first time, confirming that they are symbiotic Miras.

A comparison of the symbiotic Miras with normal Miras of similar pulsation period shows that the symbiotic stars have on average higher values of $K_0 - [12]$. This may indicate that they have higher mass-loss rates, or more likely that the dust which is being lost by the Mira is trapped within the binary system.

Key words: *binaries: symbiotic – Stars: individual: o Cet, RX Pup, V366 Car, BI Cru, SS73 38, V347 Nor, AS 210, AS 245, H 2-38, RR Tel, R Aqr, StHA 55, V335 Vul – surveys*

1. Introduction

Symbiotic stars are long-period interacting binary systems, in which an evolved red giant transfers material onto its much hotter companion, which in most systems is a white dwarf. Based on their near-IR characteristics, symbiotic stars divide into two main classes (Allen 1982) depending whether the colours are stellar (S-type) or indicate a thick dust shell (D-type). The majority ($\sim 80\%$) of catalogued systems

are S-type and have near-IR colours consistent with cool stellar photosphere temperatures of $\sim 3500 - 4000$ K. Most of them have orbital periods $\sim 500 - 1000$ days (*e.g.* Mikołajewska 2008). The near-IR colours of D-type systems indicate the presence of a dust shell which obscures the star and re-emits at longer wavelengths. IR photometric monitoring has shown that these D-type systems have large amplitude variations and that they contain Mira variables with pulsation periods in the range 300–600 days; they are often called symbiotic Miras (Whitelock 1987). Since they must accommodate the Mira with its dust shell, these D-type systems should have much longer orbital periods than the S-types, a few tens of years and more. The latest review of symbiotic Miras and a comparison with normal Miras can be found in Whitelock (2003).

Light curves of symbiotic stars reflect the very complex behaviour of these systems. They show high and low activity stages, flickering, nova-like outbursts originating from the hot component (S & D types), eclipses, ellipsoidal variability connected with orbital motion (S-type), radial pulsations (all D-type and some S-type) and semi-regular variation (S-type) of the cool component, long-term dust obscuration (mostly D-type) and other types of variability (Mikołajewska 2001).

In this paper we analyse the light curves of 13 objects that have at some time been classified as D-type symbiotics. The light-curves were provided by massive photometry surveys such as ASAS, OGLE, MACHO and near-IR monitoring at SAAO.

2. Data

Belczyński *et al.* (2000) listed coordinates for symbiotic stars, but many of these are not sufficiently accurate to identify the symbiotics unambiguously. So we first identified the 2MASS counterparts using the existing finding charts and the Aladin Java graphics interface running at the CDS in Strasbourg. This works well because symbiotic stars, which have the near-IR colours of late-type giants, are intrinsically bright in *JHK*. The 2MASS coordinates were then used to identify symbiotic stars in the OGLE, MACHO and ASAS databases.

For *o* Cet, RX Pup, V366 Car, BI Cru, SS73 38, AS 210, RR Tel, R Aqr, StHA 55, and V335 Vul, light-curves were taken from the ASAS database (Pojmański 2002)¹. These comprise *V*-band photometry obtained between November 2000 and February 2009. The ASAS *V* light-curves are illustrated in Fig. 1, while Table 1 contains the ASAS names, the mean mags (\bar{V}) and the full range of the variations found in *V* (ΔV). Although the ASAS database also contains SS73 38, there are only a few observations of it.

The OGLE-II database (Udalski *et al.* 1997)² includes a light-curve for H2-38. This comprises *I*-band photometry obtained between 1997 and 2000. The OGLE

¹official home page of ASAS project: <http://www.astro.uw.edu.pl/asas/>

²official home page of OGLE project: <http://ogle.astro.uw.edu.pl/>

I light-curve of H2-38 is shown in the second panel of Fig. 2, while Table 1 gives the OGLE name, the mean mag (\bar{I}) and the full range of the variations found in I (ΔI).

The MACHO database (Alcock *et al.* 1992)³ contains observations for H2-38, obtained between 1993 and 1999. The photometry was made through non-standard blue (B_M) and red (R_M) filters. The MACHO light-curve is shown in Fig. 2, while Table 1 gives the MACHO name, the mean mags (\bar{B}_M , \bar{R}_M) and the full range of the variations found in each band (ΔB_M , ΔR_M).

We also analyse near-IR *JHKL* photometry for *o* Cet, RX Pup, V366 Car, BI Cru, V347 Nor, SS73 38, AS 210, AS 245, RR Tel and R Aqr. This was obtained with the 0.75-m, 1.0-m and 1.9-m telescopes at SAAO and is on the system described by Carter (1990). The photometry is illustrated in Figs. 3-5 and mean magnitudes, the full range of variations and the amplitudes of pulsation estimated by fitting sinusoids to detrended light curves (see Section 3.1.1 for period derivation) are listed in Table 2. Some of the early data were published and discussed by Feast *et al.* 1983a, 1983b; Whitelock *et al.* 1983; Mikołajewska *et al.* 1999; Kotnik-Karuzza *et al.* 2006, Santander-Garcia *et al.* 2007. The near-IR magnitudes of these objects are listed in appendix table and available in electronic form at Acta Astronomica Archive⁴.

Visual light-curves for *o* Cet, RX Pup, BI Cru, AS 210, RR Tel and R Aqr were extracted from the database of the American Association of Variable Star Observers⁵, and used for comparison with the near-IR data.

Most of objects discussed here are definitely symbiotic Miras, with four exceptions; the symbiotic nature of *o* Cet, StHA 55 and V335 Vul is not certain. There have been suggestions (Jura & Helfand 1984, Kastner & Soker 2004, Ireland *et al.* 2007) that Mira B may be a low mass main-sequence (MS) star. StHA 55 and V335 Vul are only suspected of being symbiotic (Belczyński *et al.* 2000) and may well be normal C-Miras (see also Munari *et al.* 2008). AS 245 is re-classified here (section 3.1.2) as S-type symbiotic star. These objects are indicated in figures by different symbols.

3. Analysis and Results

3.1. Variability

3.1.1 Period analysis

All light-curves were analysed using the program PERIOD⁶ ver. 5.0, based on the modified Lomb-Scargle method (Press & Rybicki, 1989). Long-term trends were

³official home page of MACHO project: <http://www.macho.mcmaster.ca/>

⁴official home page of Acta Astronomica: <http://acta.astrouw.edu.pl/>

⁵official home page of AAVSO: <http://www.aavso.org/>

⁶the source program is available on <http://www.starlink.rl.ac.uk/>

Table 1: D-type symbiotic stars in optical massive surveys: designation, average magnitudes and full range of the variations (Δ) during the observation run. The first column lists the identification number of the symbiotic star from Belczyński *et al.* (2000).

No.	Name	Name in Survey	\bar{V}	ΔV	\bar{I}	ΔI	\bar{B}_M (mag)	ΔB_M	\bar{R}_M	ΔR_M
010	<i>o</i> Cet	ASAS 021920-0258.6	6.75	6.28	-	-	-	-	-	-
026	RX Pup	ASAS 081412-4142.5	12.27	1.53	-	-	-	-	-	-
030	V366 Car	ASAS 095443-2745.5	13.78	1.95	-	-	-	-	-	-
034	BI Cru	ASAS 122326-6238.3	11.44	2.90	-	-	-	-	-	-
039	SS73 38	ASAS 125126-6460.0	-	-	-	-	-	-	-	-
069	AS 210	ASAS 165120-2600.5	12.91	2.04	-	-	-	-	-	-
120	H 2-38	OGLE 180601.19-281704.2	-	-	12.21	1.73	-	-	-	-
		MACHO 105.21287.23	-	-	-	-	-9.61	>0.33	-10.78	0.96
175	RR Tel	ASAS 200419-5543.6	11.77	0.42	-	-	-	-	-	-
188	R Aqr	ASAS 234349-1517.1	8.40	5.86	-	-	-	-	-	-
s03	StHA 55	ASAS 054642+0643.8	13.01	2.90	-	-	-	-	-	-
s26	V335 Vul	ASAS 192314+2427.7	11.80	2.50	-	-	-	-	-	-

Table 2: Near-IR SAAO photometry of the symbiotic stars: average magnitudes in the $JHKL$ -bands, full range of the variation (Δ) of the $JHKL$ magnitude and the amplitudes of pulsation estimated by fitting sinusoid with peak-to-peak amplitudes of $\Delta_p J$ etc to the observations. The first column lists the identification number of the symbiotic star from Belczyński *et al.* (2000).

No.	Name	\bar{J}	\bar{H}	\bar{K}	\bar{L}	ΔJ	ΔH	ΔK	ΔL	$\Delta_p J$	$\Delta_p H$	$\Delta_p K$	$\Delta_p L$
010	ϕ Cet	-1.23	-2.10	-2.55	-3.12	1.38	1.40	1.24	1.39	1.00	1.01	0.84	0.68
026	RX Pup	5.67	4.18	2.98	2.28	3.72	3.01	2.30	1.59	1.08	1.00	0.81	0.64
034	BI Cru	7.62	6.14	4.84	3.30	2.07	1.40	1.11	0.93	0.69	0.46	0.31	0.19
030	V366 Car	7.19	5.77	4.78	3.52	3.05	2.58	1.93	1.28	0.53	0.59	0.49	0.39
039	SS73 38	9.41	7.47	5.96	4.18	3.18	2.56	1.79	1.06	0.53	0.59	0.49	0.39
060	V347 Nor	7.01	5.54	4.78	4.02	1.81	1.32	1.00	0.94	0.88	0.70	0.53	0.44
069	AS 210	9.50	7.74	6.28	4.60	2.67	2.48	1.84	1.27	1.06	1.16	1.05	0.85
105	AS 245	9.41	8.05	7.44	6.92	0.54	0.57	0.53	0.44	0.36	0.42	0.38	0.30
175	RR Tel	6.57	5.37	4.43	3.13	3.47	2.84	2.05	1.29	0.71	0.69	0.60	0.47
188	R Aqr	0.80	-0.27	-0.89	-1.72	3.58	3.07	2.42	1.79	1.00	0.91	0.78	0.72

Table 3: Pulsation periods derived from our analysis.

No.	Name	Type	ASAS	OGLE	MACHO (days)	SAAO	Other periods
010	<i>o</i> Cet	O	338±10	-	-	332±3	331.96 ¹
026	RX Pup	O	trend	-	-	575±8	578 ²
030	V366 Car	O	trend	-	-	432±6	433 ³
034	BI Cru	O	280±7	-	-	274±2	280 ⁴
039	SS73 38	C	-	-	-	463±7	
060	V347 Nor	O	-	-	-	374±4	373 ⁵
069	AS 210	C	407±14	-	-	423±7	
105	AS 245	O	-	-	-	366?	
120	H 2-38	O	-	425±36	395±16 ^a	-	
175	RR Tel	O	trend	-	-	385±4	385 ⁶
188	R Aqr	O	395±13	-	-	391±5	386.96 ¹
s03	StHA 55	C	372±15	-	-	-	395 ⁷
s26	V335 Vul	C	334±14	-	-	-	347 ⁸

^a derived from R_M .

References: [1] Kholopov 1985; [2] Mikołajewska *et al.* 1999; [3] Feast *et al.* 1983b; [4] Whitelock *et al.* 1983; [5] Santander-Garcia *et al.* 2007; [6] Kotnik-Karuza *et al.* 2006; [7] Munari *et al.* 2008; [8] Sobotka *et al.* 2003.

Table 4: New pulsation ephemerides.

No.	Name	Ephemeris
026	RX Pup	$\text{Max}(JHKL) = 2442238 + 575 \times E$
030	V366 Car	$\text{Max}(JHKL) = 2442413 + 432 \times E$
034	BI Cru	$\text{Max}(JHKL) = 2443291 + 274 \times E$
039	SS73 38	$\text{Max}(JHKL) = 2444983 + 463 \times E$
069	AS 210	$\text{Max}(JHKL) = 2446162 + 423 \times E$
120	H 2-38	$\text{Max}(R_M) = 2449205 + 395 \times E$
175	RR Tel	$\text{Max}(JHKL) = 2442207 + 385 \times E$
s03	StHA 55	$\text{Max}(V) = 24522712 + 372 \times E$

removed by subtracting a polynomial of appropriate order, and the resultant power spectra were compared with the window spectra. The periods were derived from the inverse of the maximum of the peak in the periodogram ($P = f_{max}^{-1}$), whereas their accuracy was estimated by calculating the half-size of a single frequency bin (Δf), centred on the peak (f_c is the center of the peak) of the periodogram and then converted to period units ($\Delta P = f_c^{-2} \cdot \Delta f$). The results of our period analysis are summarized in Table 3. Examples of our power spectra are shown in Fig. 6-7 and Figs. 8 shows near-IR light curves folded with pulsation periods.

The highest peak in a typical power spectrum corresponds to the pulsation period, while the other peaks represent annual aliases, second and third harmonics, long-term variation and some combination thereof. The only exceptions are the ASAS light-curve of V335 Vul, where the highest peak corresponds to the second harmonic, and the near-IR light-curves of RR Tel where it represents the annual alias. In both exceptional cases this is due to gaps in the light-curve of the object.

There is practically no difference between the power spectra derived for the *JHK* or *L* observations. They all show the same position of peaks with a little difference in power. The latter is due to differences of amplitudes of the pulsations and long-term trends in the near-IR photometry.

For four systems (AS 210, H2-38, SS73 38, and AS 245) the pulsation periods are derived for the first time. Pulsations are also detected in other systems with known periods. In particular, pulsations are always visible in the near-IR light-curves of all of the symbiotics we examined. However, the periods for *o* Cet and R Aqr (Table 3) are not as accurate as those derived from visual data collected over a few centuries (Kholopov 1985), whereas for RX Pup, V366 Car, RR Tel and BI Cru our new estimates are better than published values (Mikołajewska *et al.* 1999, Feast *et al.* 1983a, Whitelock *et al.* 1983) because they are based on more data. For some systems pulsations are also visible in the optical light-curves, although the resulting periods are less accurate than those already known (Belczyński *et al.* 2000, and references therein) because ASAS, MACHO and OGLE cover relatively short time periods (a few to several years). Finally, the optical light-curves of RX Pup, V336 Car and RR Tel do not show pulsations presumably because the Mira in these systems is obscured by optically thick dust and/or the optical light is dominated by emission from the hot component.

The near-IR measurements for AS 245 suggest significant variability and a period of the order of one year, which we adopt for the following discussion. However, with only 12 observations spread over almost two decades, the data are inadequate for a proper analysis.

Recently, Munari *et al.* (2008) estimated a pulsation period of 395 days for StHA 55 in the *V*-band. The value is very uncertain because they had only observations covering only one pulsation cycle. The pulsation period of StHA 55 derived from ASAS data, which covers 6 pulsation cycles, is 372 days.

The pulsations ephemerides for three systems for which periods are derived

here for the first time (AS 210, H2-38, SS73 38) and for StHA 55, RX Pup, V366 Car, RR Tel, and BI Cru are listed in Table 4.

Fig. 9 presents the distribution of the pulsation periods for the symbiotic Miras together with those for non-symbiotic Miras. For the symbiotic Miras we have combined the published periods (Belczyński *et al.* 2000) with our new estimates (Table 3). The data for the non-symbiotic Miras are from Olivier *et al.* (2001), and Whitelock *et al.* (1994, 2000, 2006). These non-symbiotic Miras are henceforth referred to as ‘normal Miras’, but note that they will include widely separated binary systems; indeed *o* Ceti itself is included in both the symbiotic and normal groupings. The normal Miras show distinct period distributions, with peaks at ~ 330 and ~ 530 days for the O- and C-rich objects, respectively. The period distribution for normal Miras is influenced by selection effect that are extremely difficult to quantify. We do know that there are O-rich Miras with periods over 1000 days, the OH/IR stars, but these have progenitors of several solar masses and are quite rare. The symbiotic Miras have a mean period of about 400 days, and with one exception range from 280 (BI Cru) to 580 (RX Pup). The exception, V407 Cyg, has the period of 763 days (Kolotilov *et al.* 2003) and is thought to be hot bottom burning giant (Tatarnikova *et al.* 2003) and is therefore probably more massive than its shorter period counterparts. There is no obvious difference between the periods of C-rich (5 objects) and O-rich (19 objects) symbiotic Miras. All O-rich symbiotic Miras have periods longer than the median value for their normal counterparts. Whitelock (1987) suggested that this was essentially a selection effect - mass transfer in these systems is via the stellar wind of the Mira and long period Miras have in general higher mass-loss rates. Thus symbiotic activity will be seen from white dwarfs in binary systems with longer period Miras at much larger separations than from those in binaries involving shorter period Miras, *i.e.* we expect there to be unidentified white dwarfs in binary systems with short period Miras with very low levels of interaction.

3.1.2 Long term trends

The near-IR light-curves of all symbiotic Miras included in this study show, in addition to the Mira pulsations, significant long-term variations. Such trends are very common in symbiotic Miras, and are almost certainly caused by variable dust obscuration (*e.g.* Whitelock 1987; Mikołajewska *et al.* 1999).

To get better insight into this phenomenon, we removed the Mira pulsations from the light-curves and examine the trends in the residuals. In the case of stars with periods longer than 400 days this is done by subtracting the best fitting sine-curve. For shorter period targets, *o* Cet, R Aqr, BI Cru and V347 Nor, the pulsation light-curves are asymmetrical and simply subtracting the sine-curve produced a lot of scatter in the residual. Therefore another method was used. We first generated an average pulsation curve and then subtracted it from the original light-curve. This method produced less scatter for the short period stars, while for the long

period pulsators both methods give similar results. In the case of BI Cru, data between JD2 445 400 and JD2 451 400 were used to prepare the average pulsation light-curves by excluding the dust obscuration events. In the case of R Aqr, data before JD2 444 000 were omitted from the average pulsation light-curves for the same reason.

The light-curves, prior to removal of the pulsations, are plotted in the upper panels of Figs. 3 to 5. The secular trend is clearest at J and the behaviour of $J - K$ indicates that it is due to increasing reddening, as expected for increasing optical depth of the dust. This general trend is also present in the L light-curves.

The near-IR colours of D-type systems indicate the presence of warm dust shells. Fig. 10 presents the $J - K$ vs. $K - L$ diagram for the symbiotic Miras in this study together with those for normal Miras. The symbiotic Miras are shown in both their obscured and unobscured states. This demonstrates that most of the colours can be qualitatively reproduced with a shell of around 800K (see also Whitelock 1987). In at least 50 % of the studied systems the reddening toward the Mira star was larger than reddening toward the hot component (*e.g.* Mikołajewska 1999). There appears to be very much less extinction towards the high excitation regions (emission lines and hot UV continuum) than towards the Mira suggesting that the hot component generally lies outside the dust cocoon associated with the Mira. This fact constrains the orbital separations in these systems to be $\gtrsim 10$ -15 AU, and the orbital period to be $\gtrsim 20$ yr, because the typical radius of a dust shell is $\gtrsim 5 R_{Mira}$, and the Mira radius, $R_{Mira} \sim 2$ -3 AU (Mikołajewska 1999).

In the specific case of R Aqr the obscuration was explained in terms of orbitally related eclipses of the Mira by the accreting stream (Gromadzki & Mikołajewska 2009, Willson, Garnavich & Mattei 1981). However, the dust obscuration phenomenon in symbiotic Miras cannot be, in general, orbitally related (Mikołajewska 1999). First, these events seem to occur in well observed symbiotic Miras with too great a frequency, and in several systems with more than one event observed, they were separated by $\sim 2000 - 4000$ days, much below the minimum orbital period expected for these systems. Secondly, while in RX Pup the infrared emission from the Mira shows modulation with a time scale of ~ 3000 days with two apparent minima around 1984 and 1990, at the same time the reddening towards the hot component was constant over at least 13 years (Mikołajewska *et al.* 1999). A geometry of the binary system in which the cool component is eclipsed at least twice, while the hot one is not eclipsed at all is impossible. Moreover, the fact that no D-type system exhibits greater extinction towards the hot component than towards the Mira implies that only the Mira is affected. All these point to intrinsic variations in the Mira envelope as the main cause of the dust obscuration (see Sec. 3.2.2).

For most of these systems the obscuration of light at J is not associated with a brightening at L , as might be anticipated if the dust forms in a uniform shell around the Mira (see Figs. 3 to 5). BI Cru is the one exception, but it has a spectrum quite unlike that of a normal O-rich Mira in that it does not show the characteristic H_2O

absorption. What it does show is very strong $2.3 \mu\text{m}$ CO-band emission, and in that respect it has similarities to certain B[e] stars, such as Hen 3-1138 and Hen 3-1359, (Whitelock *et al.* 1983). It is therefore possible that we are observing a slightly different phenomenon in this case. We note that all parameters derived below (distance, mass-loss rate etc) for BI Cru through relations for normal Miras must be regarded as uncertain.

C-rich Miras, including R For, also show obscuration events that cannot be reconciled with spherically symmetric dust ejection (Whitelock *et al.* 1997; Feast *et al.* . 2003; Whitelock *et al.* 2006). The alternative scenarios involve ejection around an equatorial disk or as puffs in random directions. In the cases of RR Tel and AS 210 spectro-polarimetry suggests a low inclination orbit (Schmid & Schild 2002), but they show strong dust obscuration. This fact rather favours the ejection of puffs in random directions as was suggested for C-Miras (Feast *et al.* 2003; Whitelock *et al.* 2006) and is well known among R CrB stars.

Secular trends are visible in the optical (ASAS) light-curves of RX Pup, V366 Car and RR Tel. These stars do not show pulsational variations in the visible and the trends observed are not well correlated with the long term changes in their near-IR light-curves. RR Tel and RX Pup underwent nova outbursts in the 1940s and 1970s, respectively, and the nearly linear trends in their optical light-curves are due to the fading of their hot components and nebular radiation. The cause of the optical trend in V366 Car is less clear, although the presence of a minimum with a time scale similar to the dust obscuration observed in its near-IR light-curve at earlier epochs may indicate some connection with a dust obscuration event.

The visual light-curve of α Cet shows cycle-to-cycle changes of the visual amplitude. Similar behaviour is seen in most Miras with sufficiently good light-curve coverage. Erratic variations are also evident in the near-IR data, but the coverage of the light-curves is not as good. We note, however, that the highest visual maxima are correlated with the maxima in near-IR light-curve with (see left panels of Fig. 3) which may suggest changes of the average luminosity of the Mira.

AS 245 has colours typical of an oxygen-rich Mira (see Fig. 10). However, the amplitude of the possible pulsation ($\lesssim 0.4$ mag in all bands) is lower than in other symbiotic, and even non-symbiotic, Miras. Low amplitude and uncertain pulsation suggest that the cool component of AS 245 is an SRa variable rather than the Mira. We also point out similarity between the cool giant of AS 245 and that in S-type symbiotic MWC 560 (V694 Mon). The latter also shows low-amplitude pulsations with a period of $\sim 340^{\text{d}}$ and low $K - [12]$. Gromadzki *et al.* (2007) suggested that the red component of MWC 560 is on thermally-pulsating AGB, although its pulsation characteristics may be influenced by its nearby companion possibly reducing the pulsation amplitude and the circumstellar dust. More observations are necessary to settle the nature of the cool component of AS 245, but we have enough information here to reclassify it as an S-type; its position in Fig. 10 does not show signs of the dust associated with most symbiotic Miras.

3.2. Physical parameters

The great advantage of long-period pulsating AGB stars is an opportunity to determine various physical parameters such as absolute magnitudes, distances and mass-loss rates using near-IR period-luminosity-colour relations derived by Feast, Whitelock and coworkers in a series of papers. In this section we apply these methods to estimate the physical parameters for symbiotic systems containing C-rich and O-rich Miras.

3.2.1 Extinction and distance

The absolute K magnitudes of both O- and C-rich symbiotic Miras are estimated using the latest Whitelock *et al.* (2008) period-luminosity (PL) relationship:

$$M_K = \rho[\log P - 2.38] + \delta. \quad (1)$$

The slope $\rho = -3.51 \pm 0.20$ was derived from large amplitude asymptotic giant branch variable in the LMC. We use the zero-point $\delta = -7.25 \pm 0.07$ for O-rich Galactic Miras, estimated using the revised *Hipparcos* parallaxes together with published VLBI parallaxes for OH Masers and Globular Clusters. That value agrees with those estimated for O-rich LMC Miras ($\delta = -7.15 \pm 0.06$) and C-rich Galactic ($\delta = -7.18 \pm 0.37$) and LMC ($\delta = -7.24 \pm 0.07$) Miras (assumes an LMC distance modulus of 18.39 ± 0.05 mag; van Leeuwen *et al.* 2007).

The interstellar extinction at V , A_V^D , is estimated using the Drimmel *et al.* (2003) 3-D Galactic extinction model, including the rescaling factors that correct the dust column density to account for small structures observed in the DIRBE data, but not included explicitly by the model. The extinction at JHK is then calculated from the relations given by Glass (1999) for photometry on the SAAO system. Obviously this extinction represents only the interstellar component and tells us nothing about any circumstellar reddening.

We can compare the observed $J - K$ with the intrinsic value, as discussed below, to get an estimate of the total, interstellar plus circumstellar extinction. The intrinsic $(J - K)_0$ for O Miras is estimated using the period-colour relation derived by Whitelock *et al.* (2000) for Miras in the solar neighbourhood observed by *Hipparcos*:

$$(J - K)_0 = 0.71 \log P - 0.39. \quad (2)$$

Intrinsic near-IR colours $(J - K)_0$ of C Miras are obtained from the period-colour relations for C Miras from Whitelock *et al.* (2006):

$$(J - K)_0 = 12.811 \log P - 30.801. \quad (3)$$

Although the period colour relation for O-Miras is quite well defined, at least at short periods, that for C-rich Miras is not; for example the best estimated relation, $(H - K)_0$ vs. period, has a standard deviation of $\sigma = 0.48$ mag. Therefore,

a reliable total extinction estimate is often impossible for C-rich objects and the uncertainty of the values derived for $E(B - V)$ are huge.

We assume wherever possible that the extinction derived from the period-colour relations is the total, circumstellar plus interstellar, value and that subtracting the interstellar extinction, evaluated as described above, gives the circumstellar value. The values of $E(B - V)$ in the unobscured parts of light-curves, that are used for these estimates, are listed in Table 5.

To estimate distances we derive the absolute K mag, M_K , from the period and take the observed K mag during intervals in which the objects did not show obvious dust obscuration, and average over the pulsation cycle. We use A_K derived from the colour excess to correct for the interstellar plus circumstellar extinction. The formal error of the distance derived by this approach is 12 – 20 %. The parameters derived as described above are listed in Table 4.

3.2..2 Mass loss

There is a good correlation between mass-loss rate and $K - [12]$ colour for both C- and O-rich Miras, provided we can assume that the shells are approximately spherically symmetric. This arises because to a first approximation the K and $[12]$ mags are measures of the brightness of the star and of the shell, respectively. If, however, the shell is very asymmetric and our line of site to the star is obscured by thick dust (as it would be during an obscuration event) then we will underestimate the K brightness and overestimate the mass-loss rate. With this caveat in mind we can estimate the mass-loss rates for the symbiotic Miras from their $K - [12]$ colours (Table 5).

In the case of carbon Miras, Whitelock *et al.* (2006) estimated mass-loss rates using a modification of Jura's (1987) method, and fitted an analytical formula which we use here:

$$\log \dot{M} = -7.668 + 0.7305(K - [12]) - 5.398 \times 10^{-2}(K - [12])^2 + 1.343 \times 10^{-3}(K - [12])^3. \quad (4)$$

The mass-loss rates for the symbiotic O-rich Miras are determined using the correlation with $K - [12]$ colour derived for 58 high mass-loss O-rich AGB stars in the South Galactic Cap (Fig. 21 of Whitelock *et al.* 1994).

The $[12]$ magnitudes are calculated from the *IRAS* 12-micron fluxes (Belczyński *et al.* 2000) using $[12] = -2.5 \log F_{12} + 3.62$. The K magnitudes for the objects with SAAO near-IR light-curves are the values observed outside of obvious obscuration phases and averaged over the pulsation cycle. For HM Sge and V1016 Cyg we derived the average K from their published near-IR light-curves (Taranova & Shenavrin 2000). The use of a K magnitude obtained during a dust obscuration phase could result in an overestimate of the mass-loss rate by an order of magnitude (we assume, as suggested above, that the faint phases are the result of asymmetric

obscuration and that the [12] mag remains approximately constant). For example the average K mag for V366 Car outside dust obscuration is 4.4 mag, from which we derive a mass-loss rate of $6.3 \times 10^{-7} M_{\odot} \text{yr}^{-1}$; during dust obscuration K is about 6 mag and the derived mass-loss rate is $5 \times 10^{-6} M_{\odot} \text{yr}^{-1}$. The difference is not so large for objects with greater mass-loss rates, *e.g.*, RX Pup outside of dust obscuration has $\dot{M} = 6.3 \times 10^{-6} M_{\odot} \text{yr}^{-1}$, which increases to $\dot{M} = 10^{-5} M_{\odot} \text{yr}^{-1}$ during obscuration.

For the remaining objects we use data from 2MASS (obtained between 1997 and 2000) and Munari *et al.* (1992; obtained in 1990). Whereas the near-IR data in Munari *et al.* (1992) are from SAAO using the same photometric system as the light-curves presented here, the K_s magnitudes from 2MASS have been transformed to the SAAO system using transformations from Carpenter (2001). A significant fraction of symbiotic Miras show dust obscuration events, so it is possible that some of these measurements were made during such events. Typically, for objects with SAAO near-IR light-curves, the difference between the average K and transformed 2MASS K_s is 0.1-0.2 mag, and so we adopted the average of the Munari *et al.* (1992) and transformed 2MASS values. The K magnitudes have been corrected for interstellar reddening (section 3.2..1).

We should emphasize that mass-loss rates obtained in this way are not accurate. It is also important to appreciate that we do not yet understand the obscuration events or their link to the Mira mass-losing activity. If the symbiotic stars show obscuration events for the same reason that Feast (2003) and Whitelock *et al.* (2006) have suggested that the C-Miras do, then the mass-loss will be in discreet dust puffs in random directions like RCB stars (see also Whitelock 2003). The fact that symbiotic Miras are in binary systems will almost certainly effect what happens to the dust once it leaves the immediate vicinity of the Mira in a non-random fashion, even if it does not affect the dust production itself.

Fig. 11 presents the $K_0 - [12]$ colour distribution for symbiotic Miras and compares it to those for normal Miras. The normal O-rich Miras show a distinct $K_0 - [12]$ colour distribution, which peaks at 1.76 mag, corresponding to a mass-loss rate of $\sim 10^{-7} M_{\odot} \text{yr}^{-1}$, and has a tail that extends across the region occupied by the symbiotic Miras. As can be seen from Fig. 12, a plot of the $K_0 - [12]$ colour vs. pulsation period, the tail is comprised of long period (mostly $P > 400$ days) objects. The C-rich Miras show a broad distribution from 1 to 9.5 mag which implies mass-loss rates ranging from $\sim 10^{-7}$ to $\sim 3 \times 10^{-5} M_{\odot} \text{yr}^{-1}$. The symbiotic Miras show a distinct $K_0 - [12]$ colour distribution with a peak at 4.25 mag, corresponding to a mass-loss rate of $\sim 3.2 \times 10^{-6} M_{\odot} \text{yr}^{-1}$. These figures show that the symbiotic Miras have on average larger $K_0 - [12]$ than their normal counterparts with similar periods. Fig. 13 shows a plot of $K_0 - [12]$ vs. $(J - K)_0$ for symbiotic and normal Miras. The scatter of symbiotic Miras is larger than that of the normal Miras and, although the distributions overlap, the symbiotic Miras have larger $K - [12]$ than normal Miras of the same period or same $J - K$. If this is the

result of selection effects then we are only finding symbiotic Miras at the very end of their evolution when mass-loss is at its maximum. It seems more likely to be a consequence of the binary interaction.

The widely accepted mass-loss scenario (*e.g.* Fleischer, Gauger & Sedlmayer 1992) is that the Mira pulsation lifts matter above the atmosphere, but does not accelerate it to escape velocity. As the matter falls it encounters the next pulsation, which gives it another outward impulse. Matter is pushed by pulsations until its temperature drops enough for dust to condense (at a few stellar radii). Then, radiation pressure on the dust can efficiently accelerate the dust, and the dynamically coupled gas, to the escape velocity. $K_0 - [12]$ is proportional to the amount of dust between us and the Mira, as described above. We should emphasize that in a binary system higher $K_0 - [12]$ could be the result of the lost mass not leaving the system rather than of intrinsically higher mass-loss rates. For example, if mass lost from the Mira in the binary was trapped within the system (*e.g.* near the L_4 and L_5 Lagrange points), more cool dust in the system will mean more obscuration and more flux at $12 \mu\text{m}$ and will result in higher values of $K_0 - [12]$.

An important question is about the influence of the secondary star on the mass-loss rate and its character. Podsiadlowski & Mohamed (2007) proposed a wind Roche lobe overflow (RLOF) model for *o* Cet. In their model, a slow wind from Mira fills its Roche lobe and then the matter streams – via the L1 Lagrangian point – onto an accretion disk around the companion. This model works most efficiently when the radius of dust shell is comparable with the Roche lobe radius (R_{RL}). Orbital separations for symbiotic Miras are essentially unknown, with the exception of R Aqr. The mean angular rotation rate from spectro-polarimetry suggest an average period of around 150 yr (Schmid & Schild 2002). This estimation is uncertain because their observations cover about 10 yr (only about 5% of the implied orbital period). For typical component masses, $M_{\text{hot}} \sim 0.6M_{\odot}$ and $M_{\text{Mira}} \sim 1.2M_{\odot}$, this period corresponds to an orbital separation of ~ 40 AU and $R_{\text{RL}} \sim 15$ AU. Thus wind RLOF should occur in most symbiotic Miras. Podsiadlowski & Mohamed (2007) made SPH simulations, which show that in a case similar to symbiotic Miras most of the material from the wind should be accreted or remain bound to the system, and only very small fraction is ejected to infinity, *i.e.*, the accretion rate is ~ 100 times higher than the Bondi-Hoyle value and the mass loss will tend to be confined to the orbital plane.

4. Conclusions

The study of symbiotic Miras is a difficult task because of the presence of an active accreting companion and the long time-scales of the variations (pulsation ~ 1 -2 years, dust obscuration ~ 10 years, orbital period ~ 100 yr). Fortunately data and relations estimated for normal Miras allowed us to derive some relevant physical parameters, such as distances, luminosities and order of mass-loss rates

Table 5: The physical parameters of the symbiotic stars discussed here: distance (d), mean magnitude in the K -band outside of dust obscuration phases, absolute magnitude in K -band (M_K), average $J-K$ colour ($\overline{J-K}$), unredded $J-K$ colour derived from colour-period relation ($(J-K)_0$), interstellar reddening estimated from a 3-D extinction model of Galaxy (E_{B-V}^D), total reddening estimated from colour excess (E_{B-V}), K_0 -[12] colour and logarithm of mass-loss rate ($\log \dot{M}$).

No.	Name	d (kpc)	K	M_K	$\overline{J-K}$	$(J-K)_0$ (mag)	E_{B-V}^D	E_{B-V}	K_0 -[12]	$\log \dot{M}$ ($M_\odot \text{yr}^{-1}$)
010	<i>o</i> Cet	0.11	-2.55	-7.75	1.32	1.40	0.01	-	3.04	-6.2
026	RX Pup	1.6	2.80	-8.58	2.36	1.57	0.51	1.51	4.90	-5.2
030	V366 Car	2.8	4.40	-8.15	2.07	1.48	0.59	1.13	3.06	-6.2
034	BI Cru	2.3	5.02	-7.49	2.58	1.34	0.91	2.36	4.25	-5.5
039	SS73 38	4.8	5.34	-8.27	3.09	3.40	0.76	-	3.68	-5.6
060	V347 Nor	2.9	4.78	-7.93	2.23	1.44	0.49	1.51	2.83	-6.3
069	AS 210	5.6	5.62	-8.11	2.72	2.85	0.27	-	3.43	-5.7
105	AS 245	10.2	7.44	-7.89	1.99	1.43	1.32	1.03	4.01	-5.6
120	H 2-38	7.2	6.60	-8.01	1.90	1.45	0.82	0.85	3.91	-5.7
175	RR Tel	2.5	4.18	-7.97	1.71	1.45	0.04	0.51	3.79	-5.8
188	R Aqr	0.24	-1.06	-7.99	1.59	1.45	0.02	0.23	3.38	-6.0
s03	StHA 55	3.6	5.27	-7.92	2.99	2.13	0.23	1.64	2.58	-6.1
s26	V335 Vul	3.7	5.11	-7.87	1.85	1.95	0.50	-	1.97	-6.4

(provided certain assumptions are made).

A comparison of the symbiotic Miras with normal Miras of similar pulsation period shows that the symbiotic stars have on average higher values of $K_0 - [12]$. This may indicate that they have higher mass-loss rates, or more likely that the dust which is being lost by the Miras is trapped within the binary system. Our observations do not settle this issue. Undoubtedly, mass-loss rates and mass transfer in these systems are most interesting subjects, but more observational data, especially in UV, IR and radio bands, are needed to understand it.

Acknowledgements. We are grateful to the following people who made observations from SAAO that were included in this analysis: Greg Roberts, Robin Catchpole, Brian Carter, Dave Laney and Hartmut Winkler. We also would like to thank Magda Borawska and Anna Lednicka for their work during initial phase of this project. This study made use of the American Association of Variable Star Observer (AAVSO) International Database contributed by observers worldwide and the public domain databases of The We are grateful to Michael Feast for his comments on an early draft of this paper. All Sky Automated Survey (ASAS) and The Optical Gravitational Lensing Experiment (OGLE), The Two Micron Sky Survey (2MASS), The MACHO Project (MACHO) which we acknowledged. This research has made use of the SIMBAD database, operated at CDS, Strasbourg, France. This work was partly supported by the Polish Research Grants No. 1P03D 017 27 and N203 395534.

REFERENCES

- Alcock *et al.* 1992, in *"Robotic Telescopes in the 1990s"*, ed. A.V. Fillipenko, ASP Conf. Ser. No. 34, p.193.
- Allen, D.A. 1982, in: *The nature of symbiotic stars, Reidel (Dordrecht)*, , 27.
- Belczyński, K., Mikołajewska, J., Munari, U., Ivison, R. J. and Friedjung, M. 2000, *A&AS*, **146**, 407.
- Carpenter, J.M. 2001, *AJ*, **121**, 2851.
- Carter, B.S. 1990, *MNRAS*, **242**, 1.
- Drimmel, R., Cabrera-Lavers, A., and López-Corredoira, M. 2003, *A&A*, **409**, 205.
- Feast, M.W., Whitelock, P.A., Catchpole, R.M., Roberts, G., and Carter, B.S. 1983a, *MNRAS*, **202**, 951.
- Feast, M.W., Catchpole, R.M., Whitelock, P.A., Carter, B.S., and Roberts, G. 1983b, *MNRAS*, **203**, 373.
- Feast, M.W., Whitelock, P.A., and Marang, F. 2003, *MNRAS*, **346**, 878.
- Feast, M.W., Whitelock, P.A., and Menzies, J.W. 2006, *MNRAS*, **369**, 751.
- Fleischer, A., Gauger, A., and Sedlmayer, E. 1992, *A&A*, **266**, 321.
- Glass, I.S. 1999, *Handbook of Infrared Astronomy*, , CUP.
- Gromadzki, M., and Mikołajewska, J. 2009, *A&A*, **495**, 931.
- Gromadzki, M., Mikołajewska, J., Whitelock, P.A., and Marang, F. 2007, *A&A*, **463**, 703.
- Ireland, M.J., Monnier, J.D., Tuthill, P.G., and *et al.* 2007, *ApJ*, **662**, 651.
- Jura, M. 1987, *ApJ*, **313**, 743.
- Jura, M. and Helfand, D.J. 1984, *ApJ*, **287**, 785.
- Kastner, J.H. and Soker, N. 2004, *ApJ*, **616**, 1188.

- Kholopov, P.N. 1985, *General Catalogue of Variable Stars*, fourth edition, Nauka, Moscow.
- Kolotilov, E.A., Shenavrin, V.I., Shugarov, S.Yu., and Yudin, B.F. 2003, *Astron. Rep.*, **47**, 777.
- Kotnik-Karuza, D., Friedjung, M., Whitelock, P.A., and *et al.* 2006, *A&A*, **452**, 503.
- van Leeuwen F., Feast M.W., Whitelock P.A., and Laney C.D. 2007, *MNRAS*, **379**, 723.
- Mikołajewska, J. 1999, in *"Optical and Infrared Spectroscopy of Circumstellar Matter"*, eds. E. Guenther, B. Stecklum, and S. Klose, ASP Conf. Ser. 188, p.291.
- Mikołajewska, J. 2001, in *"Small-Telescope Astronomy on Global Scale"*, eds. B. Paczyński, W.P. Chen & C. Lemme, ASP Conf. Ser. 246, p. 167.
- Mikołajewska, J. 2004, in *"Compact Binaries in the Galaxy and Beyond"*, IAU Coll. No. 194, ed. G. Tovmassian & E. Sion, Revista Mexicana de Astronomía y Astrofísica, Vol. 20, p.33.
- Mikołajewska, J. 2007, *Balt. Astron.*, **16**, 1.
- Mikołajewska, J., Brandi, S., Hack, W., and *et al.* 1999, *MNRAS*, **305**, 190.
- Munari, U., Yudin, B.F., Taranova, O.G., and *et al.* 1992, *A&AS*, **93**, 383.
- Munari, U., Siviero, A., Graziani, M., and *et al.* 2008, *Balt. Astron.*, **17**, 301.
- Olivier, E.A., Whitelock, P., and Marang, F. 2001, *MNRAS*, **326**, 490.
- Posiadłowski, P., and Mohamed, S. 2007, in *"Evolution and chemistry of symbiotic star, binary post-AGB and related objects"*, eds. J. Mikołajewska & R. Szczerba, Baltic Astronomy, 16, 26.
- Pojmański, G. 2002, *Acta Astron.*, **52**, 397.
- Press, W.H. and Rybicki, G.B. 1989, *ApJ*, **338**, 277.
- Sobotka, P., Pejcha, O., Šmelcer, L., and Marek, P. 2003, in *"Symbiotic Stars Probing Stellar Evolution"*, ASP Conference Proceedings, eds. R.L.M. Corradi, J. Mikołajewska and T.J. Mahoney, p.171.
- Schmid, H.M. and Schild, H., 2002, *A&A*, **395**, 117.
- Taranova, O.G. and Shenavrin, V.I. 2000, *Astronomy Letter*, **26**, 600.
- Tatarnikova, A. A., Marrese, P. M., Munari, U., and *et al.* 2003, *MNRAS*, **344**, 1233.
- Udalski, A., Kubiak, M., and Szymański, M. 1997, *Acta Astron.*, **47**, 319.
- Willson, L.A., Garnavich, P. and Mattei, J.A. 1981, *IBVS*, **1961**, .
- Whitelock, P.A. 1987, *PASP*, **99**, 573.
- Whitelock, P.A. 1988, *The Symbiotic Phenomenon, Proceedings of IAU Colloq. 103*, eds. J. Mikołajewska *et al.* , Kluwer Academic Publishers (ASSL, Vol. 145), p.47.
- Whitelock, P.A. 2003, in *"Symbiotic Stars Probing Stellar Evolution"*, ASP Conference Proceedings, eds. R.L.M. Corradi, J. Mikołajewska and T.J. Mahoney, p.41.
- Whitelock, P.A. & Feast, M.W. 2000, *MNRAS*, **319**, 759.
- Whitelock, P.A., Feast, M., Roberts G., Carter, B. and Catchpole R. M. 1983, *MNRAS*, **205**, 1207.
- Whitelock, P.A., Menzies, J., Feast, M., and *et al.* 1994, *MNRAS*, **267**, 711.
- Whitelock, P.A., Marang, F. and Feast, M.W. 2000, *MNRAS*, **319**, 728.
- Whitelock, P.A., Feast, M.W., Marang, F., and Groenewegen, M.A.T. 2006, *MNRAS*, **369**, 751.
- Whitelock, P.A., Feast, M.W., and van Leeuwen, F. 2008, *MNRAS*, **386**, 313.

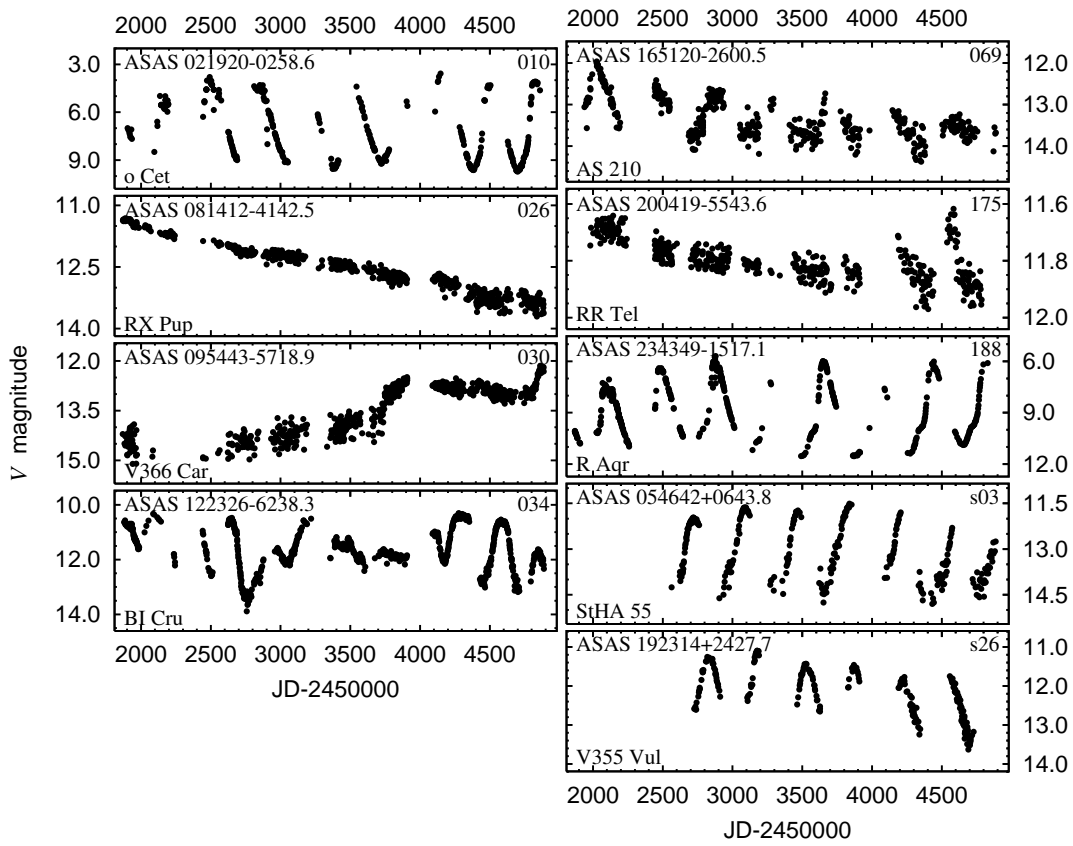


Figure 1: ASAS light curves of type-D symbiotic stars.

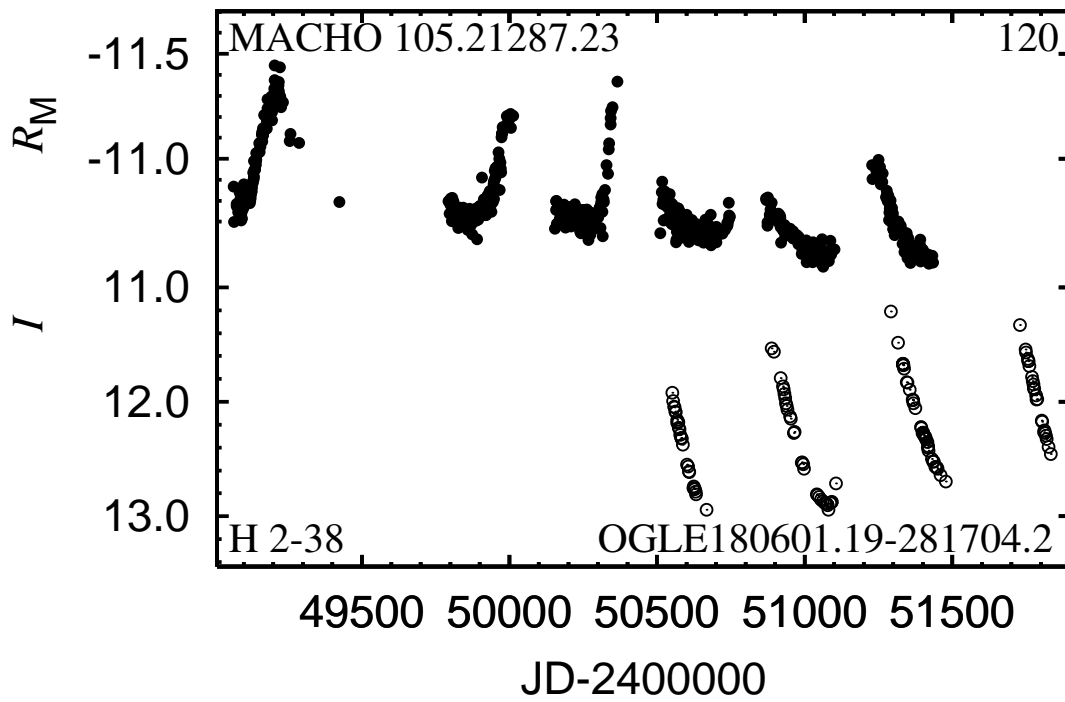


Figure 2: MACHO (filled circle) and OGLE (open circle) light curve of H 2-38.

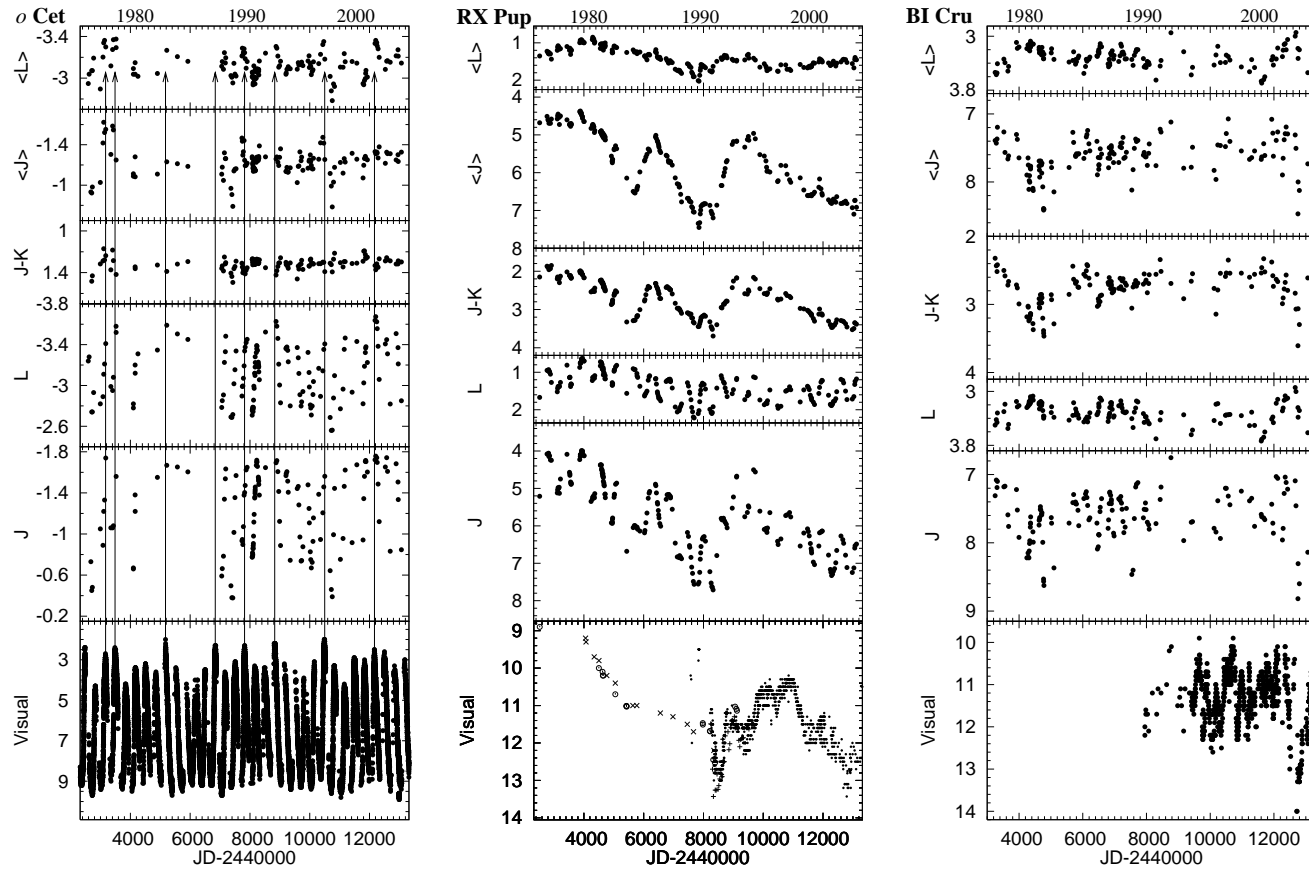


Figure 3: Near-IR light curves of *o* Cet (left panels), RX Pup (middle panels) and BI Cru (right panels). In left panels arrows mark maxima.

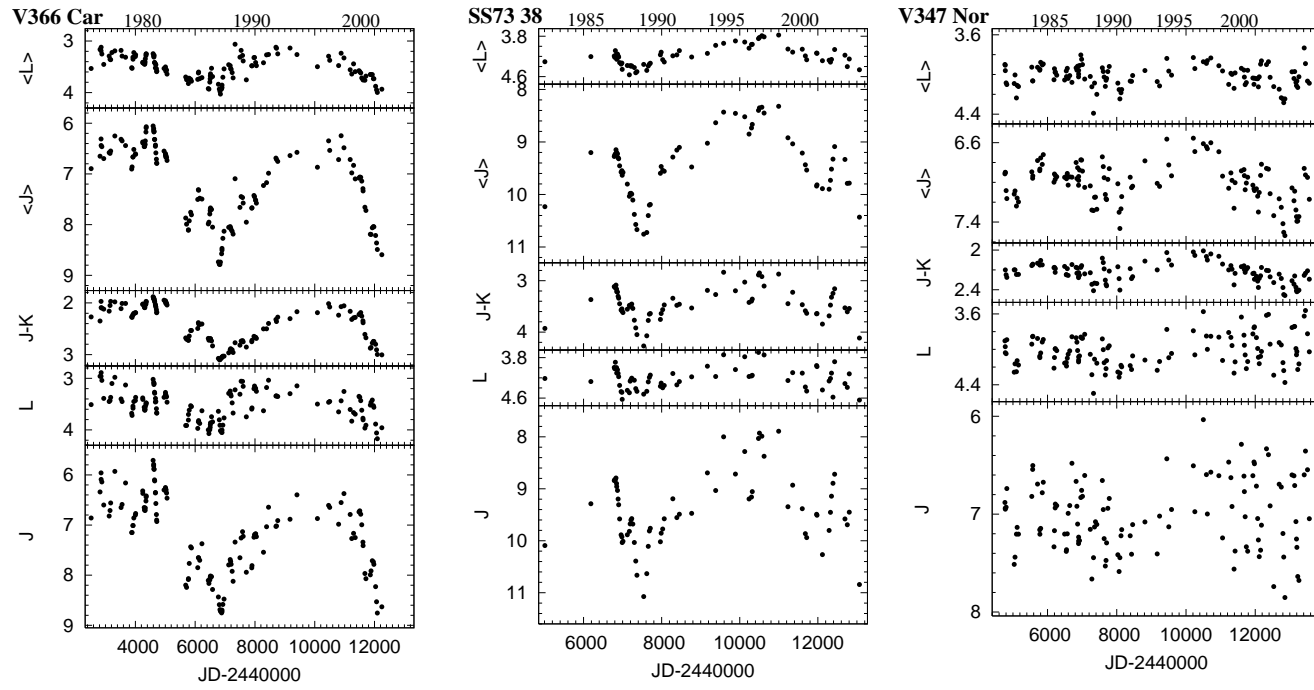


Figure 4: Near-IR light curves of V366 Car (left panels), SS73 38 (middle panels) and V347 Nor (right panels).

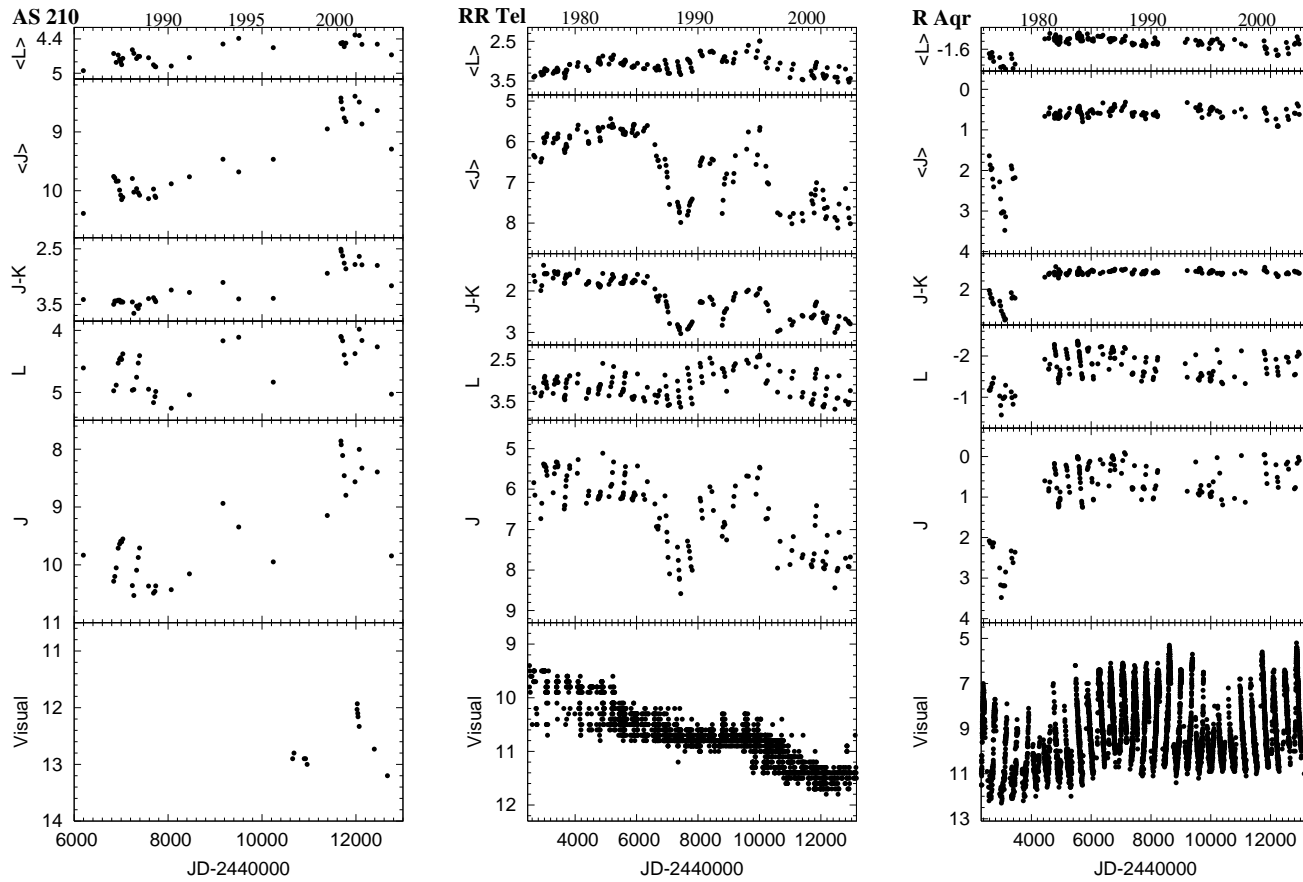


Figure 5: Near-IR light curve of AS 210 (left panels), RR Tel (middle panels) and R Aqr (right panels).

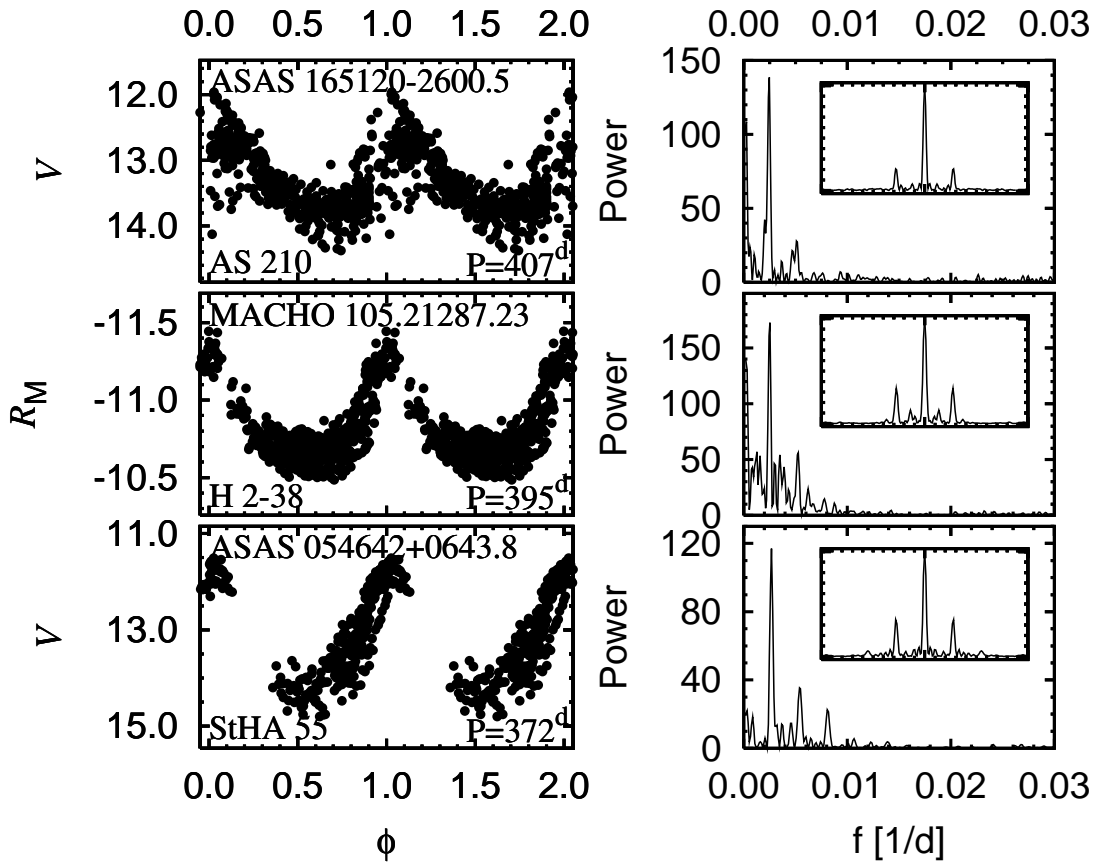


Figure 6: Light curves of AS 210, H 2-38 and StHA 55 folded with pulsation periods (left panels) and related power spectra (right panels). Insights in top right corners of power spectra panels show power spectrum of windows.

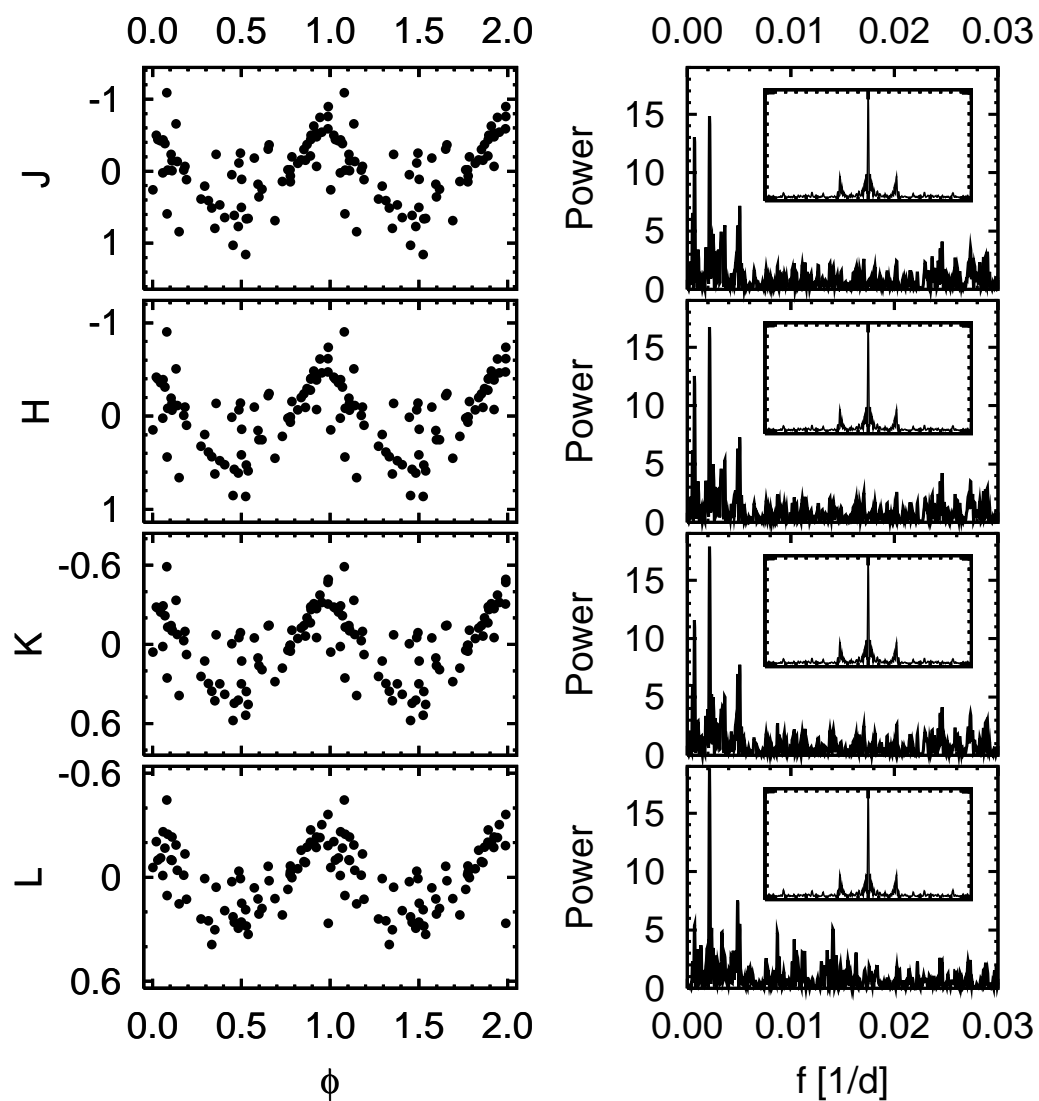


Figure 7: Near-IR light curves of SS73 38 folded with pulsation periods (left panels) and related power spectra (right panels). Insights in top right corners of power spectra panels show power spectrum of windows.

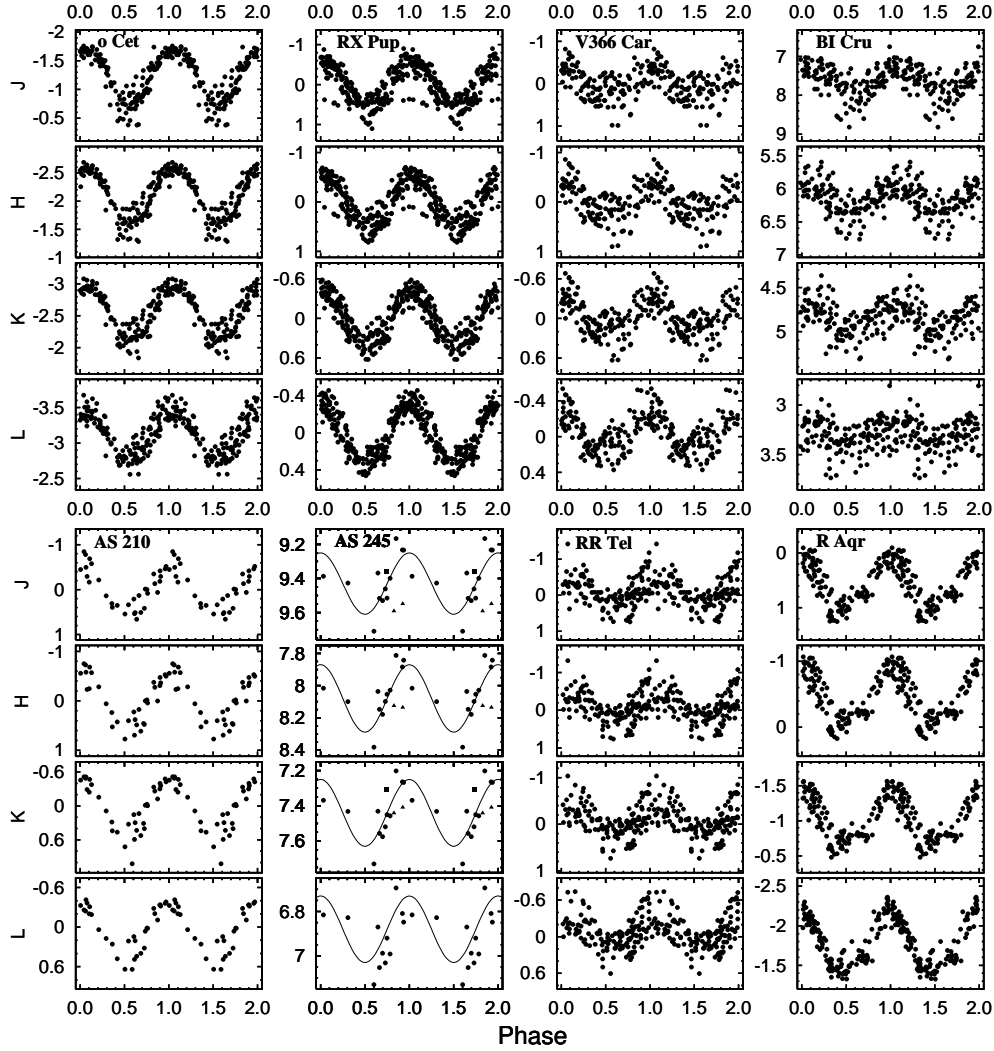


Figure 8: Near-IR light curves of studied objects folded with pulsation periods. Ephemerides from Table 4 are used for most objects with the exception of *o* Cet and R Aqr. In case of these object ephemerides are taken from Kholopov 1985. In panels of AS 245 dots represent SAAO data, triangle 2MASS, squares DENIS.

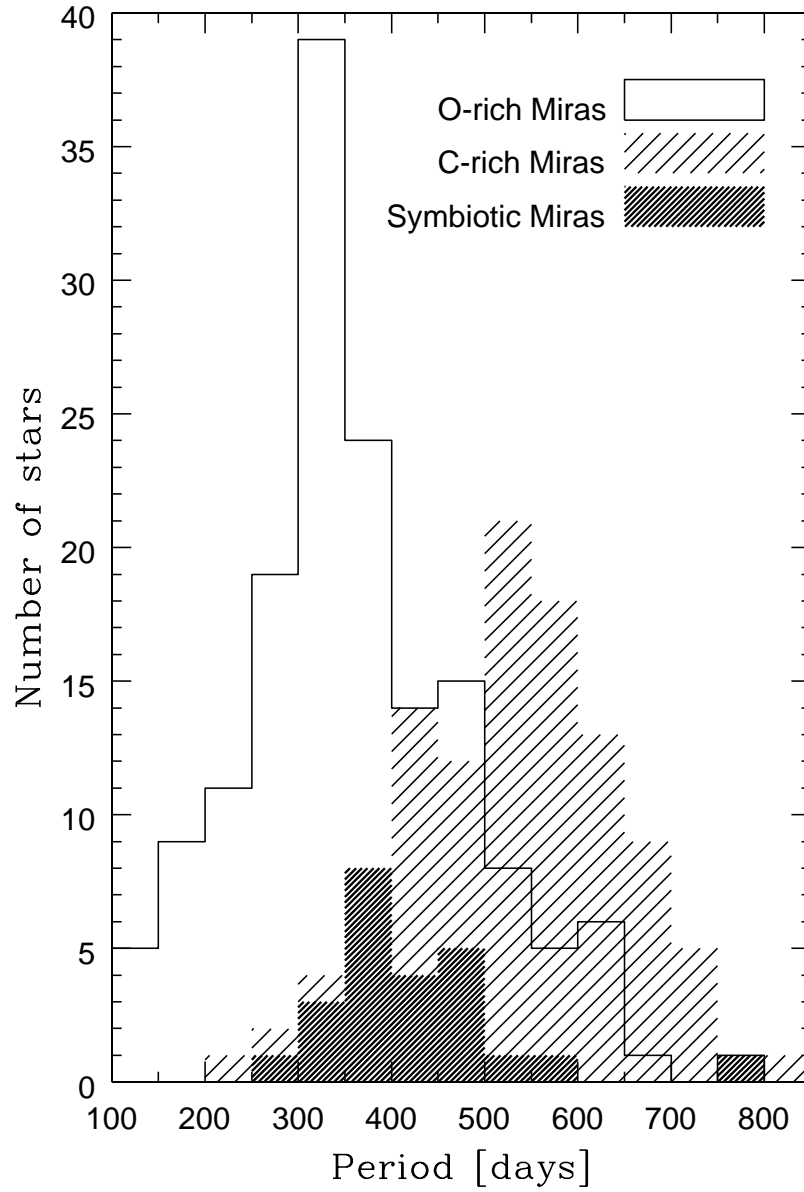


Figure 9: The pulsation period distribution for symbiotic Miras together with those for normal field Miras (Olivier *et al.* 2001, Whitelock *et al.* 1994, 2000, 2006).

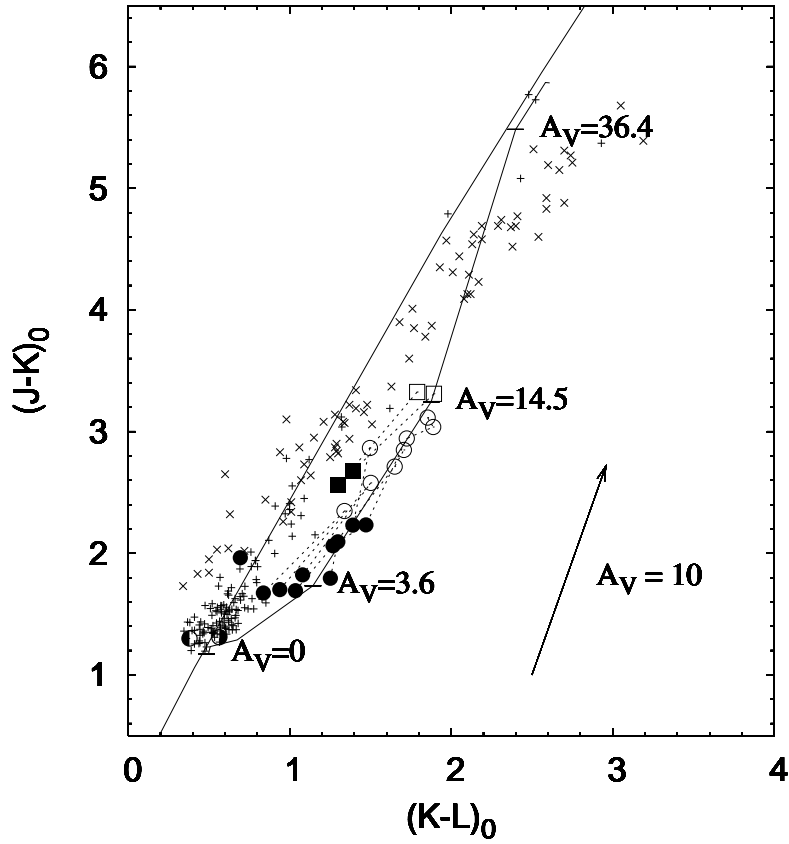


Figure 10: The $(J-K)_0$ vs. $(K-L)_0$ colour-colour diagram. Colours are deredded using extinction from galactic 3-D model. Open dots represent oxygen rich symbiotic Miras during dust obscuration, filled dots outside obscuration. Open squares represent carbon rich symbiotic Miras during dust obscuration, whilst filled outside obscuration. For comparison we also plot colours of oxygen rich Miras (+) and carbon rich Miras (\times). For objects with uncertain nature different symbols were used: \circ Cet (\odot), AS 245 (\bullet). Straight line shows black body colours. Simple model of star with shell dust is plot as well. The temperature of star is 2750 K (black body), whilst dust shell temperature is 800 K. This model also includes line blanketing.

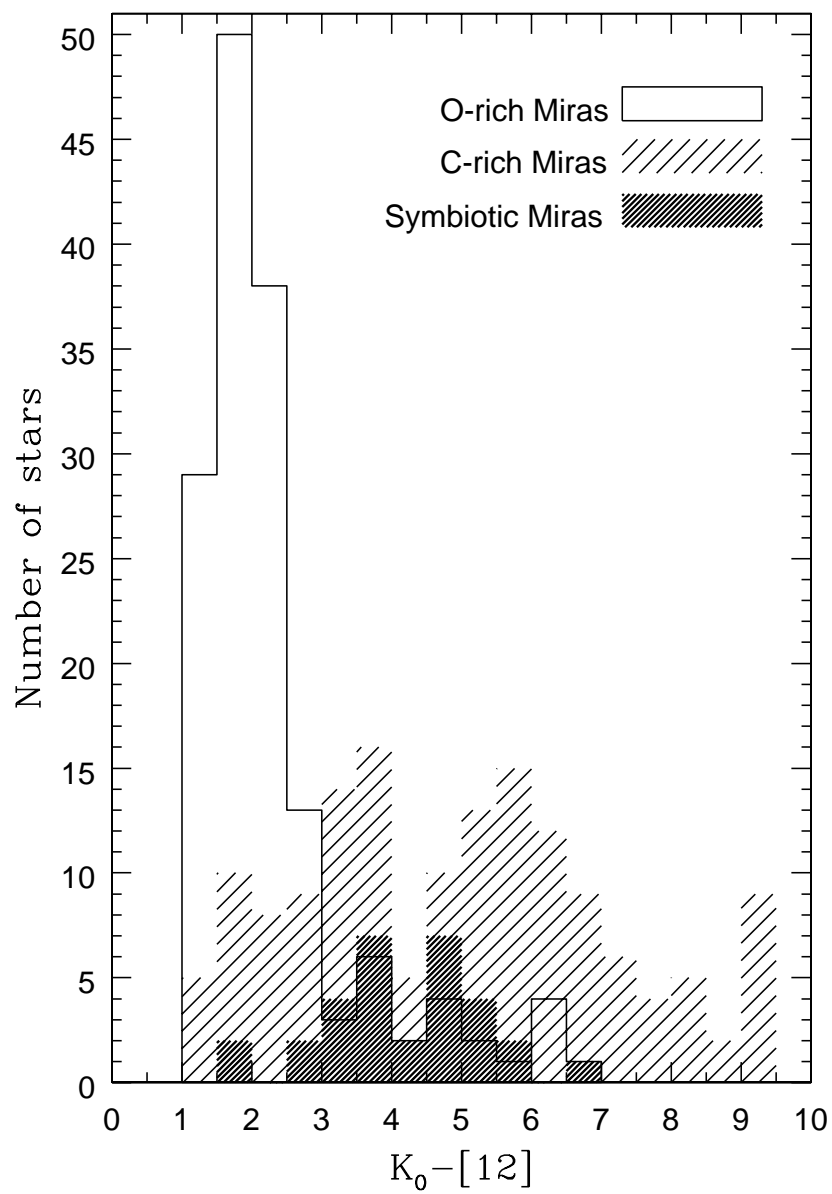


Figure 11: $K_0 - [12]$ distribution for symbiotic Miras together with those for normal Miras.

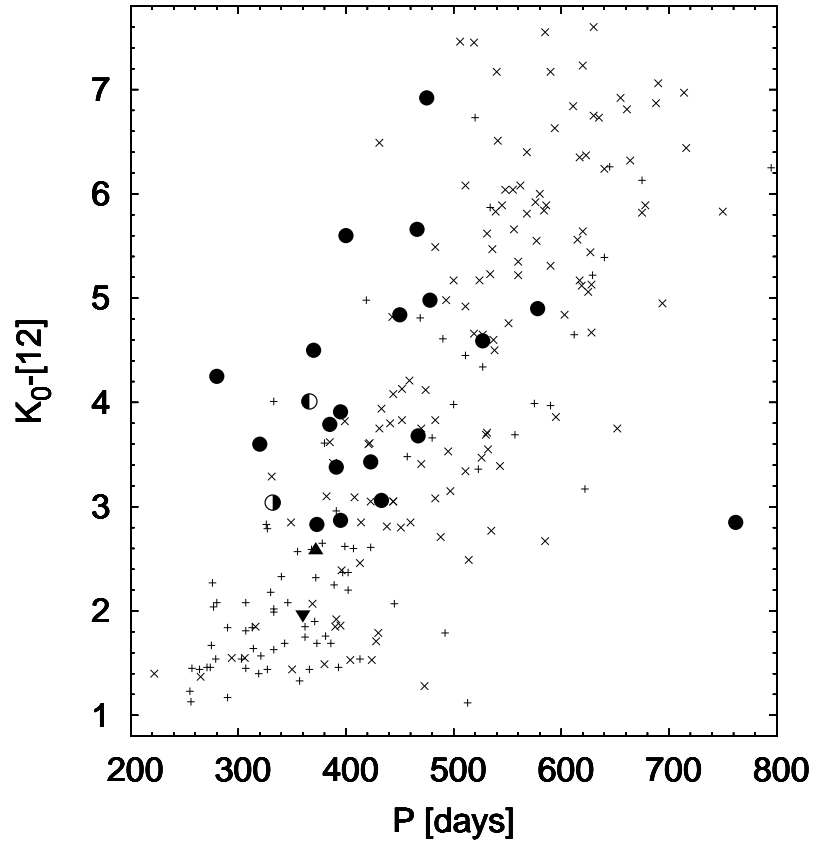


Figure 12: Pulsation period vs. $K_0 - [12]$ colour for symbiotic Miras (\bullet). For comparison we also plot colours of oxygen rich Miras ($+$) and carbon rich Miras (\times). For objects with uncertain nature different symbols were used: o Cet (\circ), AS 245 (\bullet), StHA 55 (\blacktriangle), and V335 Vul (\blacktriangledown). The discrepant point at $P=763$ days is V407 Cyg, which is thought to be hot bottom burning giant and significantly more massive than the other symbiotic Miras (see text for detail).

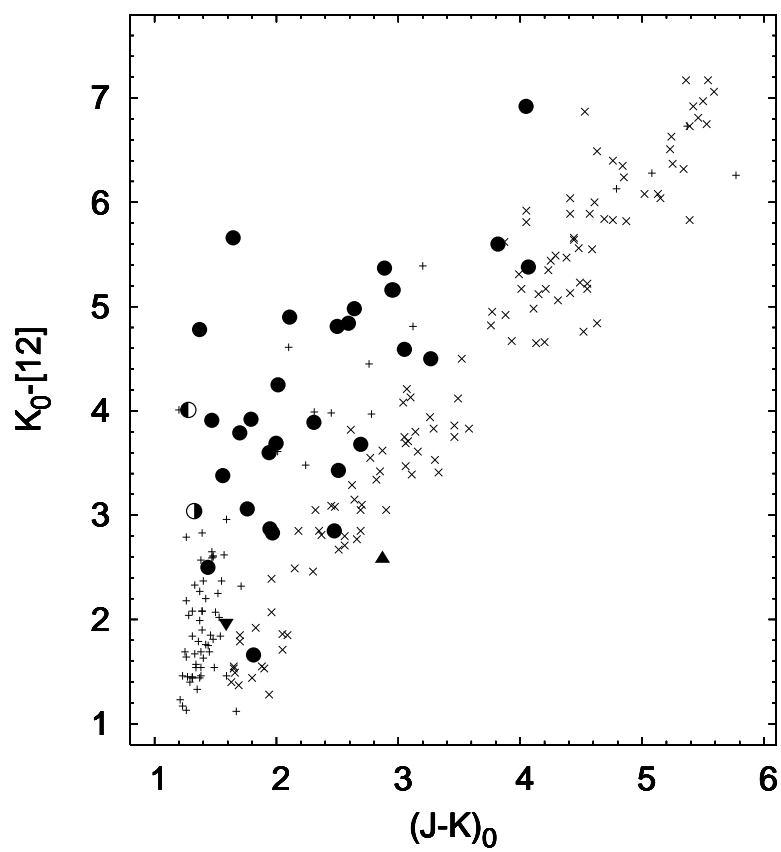


Figure 13: $(J-K)_0$ vs. $K_0-[12]$ colour for symbiotic Miras (\bullet). For comparison we also plot colours of oxygen rich Miras (+) and carbon rich Miras (\times). For objects with uncertain nature different symbols were used: \circ Cet (\odot), AS 245 (\ominus), StHA 55 (\blacktriangle), and V335 Vul (\blacktriangledown).